







Study of aluminum nitride films deposited on silicon for fabrication of MEMs devices

Estudo dos filmes de nitreto de alumínio depositados sobre silício para fabricação de MEMs

Péricles Lopes Sant'Ana^{1,*} , Argemiro Soares da Silva Sobrinho¹ , Julio Cezar Faria¹, Douglas Marcel Gonçalves Leite¹ , André Luis de Jesus Pereira¹ , Newton Adriano dos Santos Gomes¹

1. Departamento de Ciência e Tecnologia Aeroespacial – Instituto Tecnológico de Aeronáutica – São José dos Campos (SP), Brazil.

Correspondence author: drsantanapl@gmail.com

Section Editor: Maria Lúcia P Silva

Received: Dec. 09, 2020 **Approved:** Jan. 26, 2021

ABSTRACT

In this work, aluminum nitride (AlN) thin films deposited on the silicon (100) by RF magnetron-sputtering were analyzed. Nitrogen and argon plasmas were used in a vacuum system technique, being possible to obtain films oriented to the (002) crystallographic direction analyzed by X-ray diffraction (XRD) technique. Scanning electronic microscopy (SEM) was used to obtain the chemical composition (% at.) of AlN thin films. SEM analyses were accomplished to verify the images of the AlN films. Raman spectroscopy was used to obtain the Raman displacement as a function of the light intensity of the beam incident on the AlN films. Therefore, it was possible to reach the peaks of laser radiation absorption ($\lambda = 514 \text{ nm}$) during Raman scattering. Ellipsometry was required to obtain: the roughness (Rz), optical gap (E_{0d}), and films thickness. Optical properties of the films depend on the temperature during the deposition. COMSOL software was required to simulate the performance of MEMS device, operating in the match circuit on a few ten of MHz resonance frequency.

KEYWORDS: RF magnetron sputtering, Aluminum nitride thin films, Structural properties, Raman Spectroscopy, Ellipsometry, COMSOL.

RESUMO

Neste trabalho, analisaram-se filmes finos de nitreto de alumínio depositados sobre o silício (100) por RF *magnetron sputtering*. Plasmas de nitrogênio e argônio foram usados em um sistema de vácuo, sendo possível obter filmes orientados na direção cristalográfica (002), analisados pela técnica de difração de raios X (DRX). A microscopia eletrônica de varredura foi usada para obter as imagens dos filmes de AlN, e a espectroscopia Raman, para obter o deslocamento Raman em função da intensidade de luz do feixe incidente nos filmes de AlN. Dessa forma, puderam-se obter os picos de absorção de radiação do *laser* ($\lambda = 514 \text{ nm}$) durante o espalhamento Raman. A elipsometria foi requerida para obter a rugosidade (Rz), o *gap* óptico (E_{0d}) e a espessura dos filmes. As propriedades ópticas dos filmes analisados dependem da temperatura durante a deposição. Usou-se o programa COMSOL para simular o desempenho dos dispositivos de microscopia eletrônica de varredura operando em um circuito de poucas dezenas de MHz de frequência de ressonância.

PALAVRAS-CHAVE: RF *magnetron sputtering*, Filmes finos de AlN, Propriedades estruturais, Espectroscopia Raman, Elipsometria, COMSOL.

INTRODUCTION

The III-V nitrides are potential candidates for optoelectronic applications owing to their direct and broadband gaps. Among them, aluminum nitride (AlN) is the most interesting compound¹, with a wide band of band, high values of



surface acoustic speed, thermal conductivity, dielectric constant, and stability and hardness at high temperatures². For these and other reasons, AlN is a potential candidate for use in the manufacture of microelectromechanical systems (MEMs), including those ones using surface acoustic waves (SAWs)³.

Among all piezoelectric materials, AlN has become very popular in resonator application owing to its high electrical resistivity, homogeneous grain nucleation along the c axis and constant piezoelectric performance throughout the operating frequency². In the latter field particularly, the ability to deposit high-quality films on silicon substrates by spraying at low temperature³ allowed the manufacture of chip integrated signal filters for telecommunication devices in the ultra-high frequency (UHF) regime, based on MEMs devices⁴. High-quality epitaxial AlN films on suitable substrates are essential for this application.

The objective of this work was to study the effects of different conditions of deposition times and temperature of the sample holder, on the AlN films microstructure, keeping the pressure, flow of argon and nitrogen gases and the power of the electrical discharge of the radio frequency fixed, besides evaluating the optical properties of these films under visible light by ellipsometry. Ultimately, it was used COMSOL Multiphysics, to simulate a starting circuit coupled to AlN deposited on silicon, operating in resonance in the frequency range of MHz.

DEPOSITION SYSTEM AND EXPERIMENTAL CONDITIONS

The silicon sheets (100) previously conditioned in a vacuum pack were inserted inside a reactor to receive the coating of AlN in the form of thin films. In order to grow the AlN films in a stainless-steel chamber, it was proposed to design and manufacture the chamber, commonly (reactor) with a cylindrical shape diameter of 65 cm and height of 50 cm. A solid electrode disc with the target of Al (99.99%) of 5 inches with distance of 5 cm from substrates was used.

This system is installed at the Laboratório de Plasmas e Processos of Instituto Tecnológico de Aeronáutica (ITA), and consists of a primary mechanical pump (model E2M-18, manufactured by Edwards company) and a diffuser pump (Diffstak, Edwards) with the pump rate of 1,500 L/s. The diffuser pump is cooled by a system with continuous water circulation. The residual pressure achieved by this system is in the order of 10⁻⁶ Torr. The deposition pressure of the films was measured using a Baratron meter (manufactured by MKS company), and the residual pressure by a gauge ion meter (Edwards). The bottom pressure of the chamber measured for all depositions was 4.0 × 10⁻⁶ Torr.

The reactor has four gas lines, and it is possible to control the flow of the two gases independently, through a MKS controller model 247C. As precursors, a metallic aluminum target with 99.9% purity, argon gas and nitrogen gas was used.

The control of gas injection was carried out by two independent flow meters of the MKS model 1179. The plasma discharge was sustained by a radiofrequency (RF) generator of maximum power of 1,200 W operating at fixed frequency (13.56 MHz, ENI-model ACG-10B), connected in serial with an impedance matching circuit (Plasma-Therm, 12/NJ). A power controller manufactured under the proportional integral derivative (PID) logic was coupled to the reactor, being responsible for supplying thermal energy to the interior of the chamber. Thus, the temperature values ranged from 200 to 350°C, which were programmed in some depositional series.

Before starting the thin films deposition, a cleaning procedure for the aluminum target (pre-sputtering) was carried out by 20 minutes using only argon to ensure that the target surface was cleaned at the time of deposition. Tab. 1 shows the conditions.

Table 1: Deposition parameters of aluminum nitride films grown by RF magnetron sputtering on Silicon (100) sheet substrates at base pressure of 4.5 × 10⁻⁶ Torr. The argon flow was kept constant at 3 SCCM, the nitrogen flow at 7 SCCM, at an RF power of 200 W and at a pressure of 2 mTorr.

Sample	Temperature of sample holder (°C)	Deposition time (min)
1	P.T.	180
2	P.T.	200
3	350	240
4	P.T.	240
5	350	360
6	350	280

RF: radiofrequency; P.T.: plasma temperature.

RESULTS

X-ray diffraction

The structural characterization of the thin films was performed by means of X-ray diffraction (XRD) measurements, as shown in the diffractogram of Figs. 1 and 2, provided by the software of equipment, the Panalytical X'Pert3 Powder, using the powder method. XRD measurements were performed in the Bragg-Brentano configuration with a detection range between 10° and 65° . The wavelength used was 1.54 \AA (Cu K α).

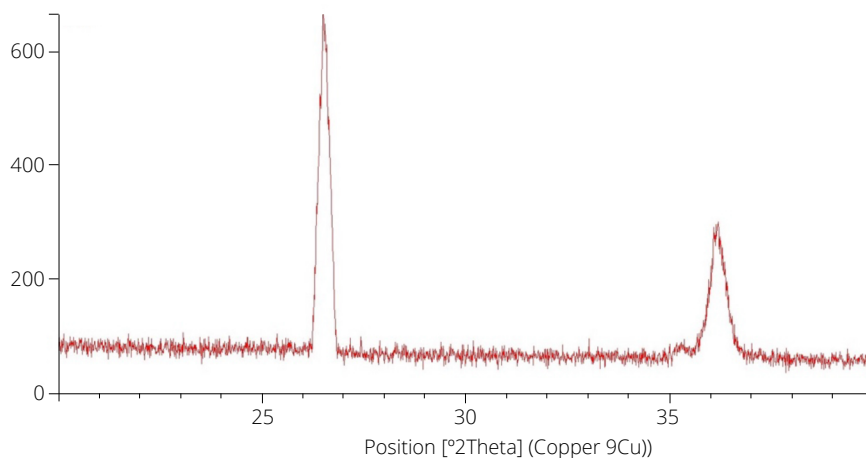


Figure 1: Diffractogram obtained by powder method for scanning from 20° to 40° on the sample 3 of aluminum nitride (350°C, 240 min) at a base pressure of 4.5×10^{-6} Torr. The argon flow was kept constant at 3 SCCM, the nitrogen flow at 7 SCCM, at a radiofrequency (RF) power of 200 W and pressure at 2 mTorr.

Generally, AlN thin films seen in the literature have intense and acute peaks associated with angles above 30° . In this period, it was tried to grow films with preferential direction (002) associated with the angle of 36.2° .

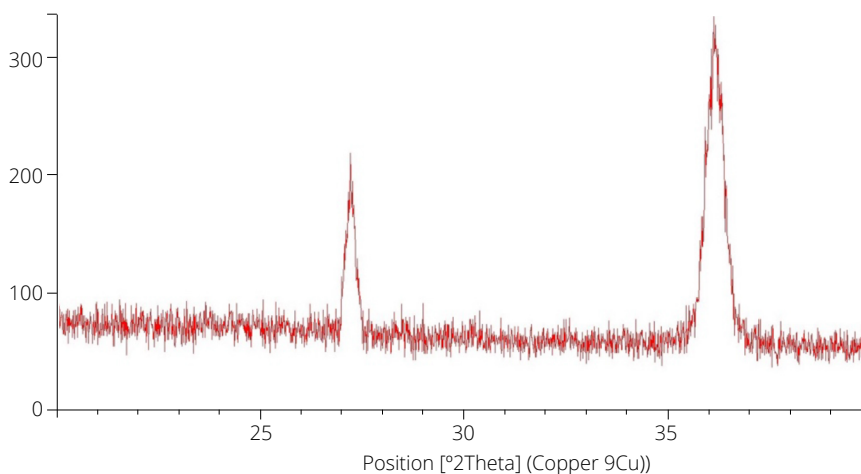


Figure 2: Diffractogram obtained by the powder method, for scanning from 20° to 40° on aluminum nitride sample 4 (plasma temperature, 240 min) at pressure of 4.5×10^{-6} Torr. The argon flow was kept constant at 3 SCCM, the nitrogen flow at 7 SCCM, at a radiofrequency (RF) power of 200 W and pressure at 2 mTorr.

Peaks were identified at positions $2\theta = 26.6^\circ$ (the most intense and acute) and $2\theta = 36.02^\circ$ in sample 3 (350°C, 240 min), and the peaks at $2\theta = 27.2^\circ$ and $2\theta = 36.2^\circ$ (more intense and acute) pointed out that the films are polycrystalline. Peaks $2\theta = 36.2^\circ$ indicated the crystallographic direction (002), and the other peaks were not associated with a well-defined crystallographic direction. They were probably associated with some random or unknown orientation. For the preferred growth direction in the plane (002), the tabulated network spacing value $d_{002} = 2.49$ angstroms was associated.

The peak of grain size was calculated using the XRD technique, which provided an estimate of the average crystallite size of 1.106 μm . It was also found that films grown with better crystallographic properties correspond to the films deposited with a greater flow of N_2 compared to argon. So far, all samples had peaks related to hexagonal AlN (P63mc, Space Group (GP) 186), both samples grown on glass and those grown on Si (100).

Particles with dimensions less than 1 μm may show diffracted intensities at values of 2θ slightly above or below the value of the Bragg angle, due to the peak widening effect. Thus, the Bragg angle (θ) of the peak apex and the width at half height of the peak (FWHM), represented by β , were determined. Applying the data obtained in the Scherrer formula⁵, described in Eq. 1, it was suggested to determine the value of the average grain size (τ) for AlN thin films.

$$\tau = \frac{K\lambda}{\beta \cos \theta} \tag{1}$$

in which: K = a form factor; λ = the X-ray wavelength; β = the width value at half height of the XRD peak (FWHM), in radians; θ = the Bragg angle.

Generally, the form factor has a typical value for AlN thin films: $K = 50,99$ (constant); $\lambda = 1,54 \text{ \AA}$; $\beta = 0,057 \pm 0,001$; $\theta = 36,6^\circ$.

The calculations provided an average grain size of $1.03 \times 10^{-6} \text{ m}$.

Further on, it is worth reporting that a possibility of structural alteration that can occur in plasma depositions is the hydrophilization of the most superficial region of the material. This process can promote atoms by diffusion of water vapor present in the atmosphere. This diffusion mechanism occurs more intensely in the amorphous or semicrystalline regions of the material, and can house atoms between the hexagonal cells, mainly in the crystallographic plane (002), which interface with the set of cells contained in the plane (001) or even on the surface in which atoms have greater mobility.

This discussion becomes significant if we consider that samples 3 (350°C, 240 min) and 4 (plasma temperature, 240 min) showed the diffractogram assignments for the films that presented 36.6° angle for the plane (002) and 27.3° angle, although associated with an undesirable direction for the film, which pointed out intense and well-defined peaks, as revealed by the partial results of the XRD of the samples in question. Thus, it appears that the diffusion of oxidative or oxygen-containing groups occurs in preferential locations within the bulk of the films, despite the fact that it happens in very low proportions, since the AlN thin film is dense and resistant to oxidation or penetration of oxidizing groups even at high temperatures.

Scanning electronic microscopy

The chemical composition of AlN films was investigated by X-ray dispersive energy (X-rayDE) measurements coupled to a scanning electron microscope (SEM) manufactured by JEOL company. This microscope provides information about the topographic structure and the surface chemical composition. Figures 3 and 4 show the SEM images of AlN thin films deposited in different conditions of temperature and deposition time. The argon flow was kept constant at 3 SCCM, the nitrogen flow at 7 SCCM, at an RF power of 200 W and pressure at 2 mTorr.

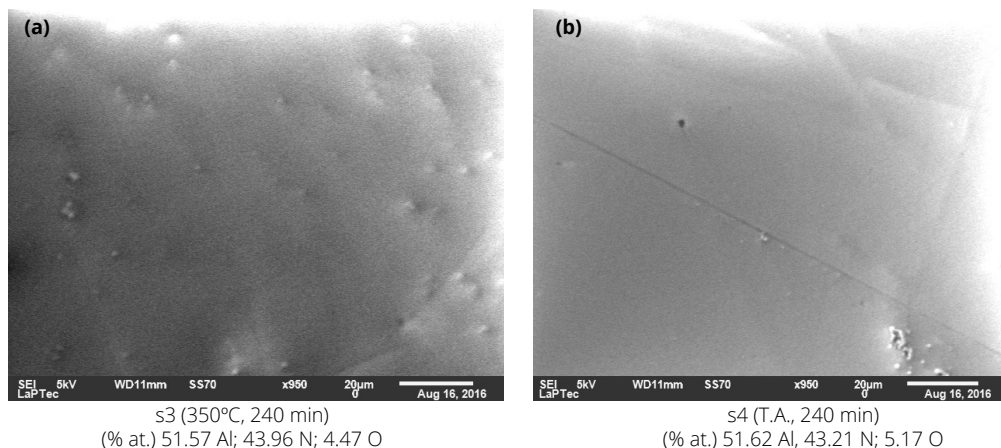


Figure 3: Scanning electron microscopy images for aluminum nitride (AlN) samples 3 (a, s3) and 4 (b, s4) generated at 2 kV, $\times 950$ magnification, 20-micron area and 11-mm working distance.

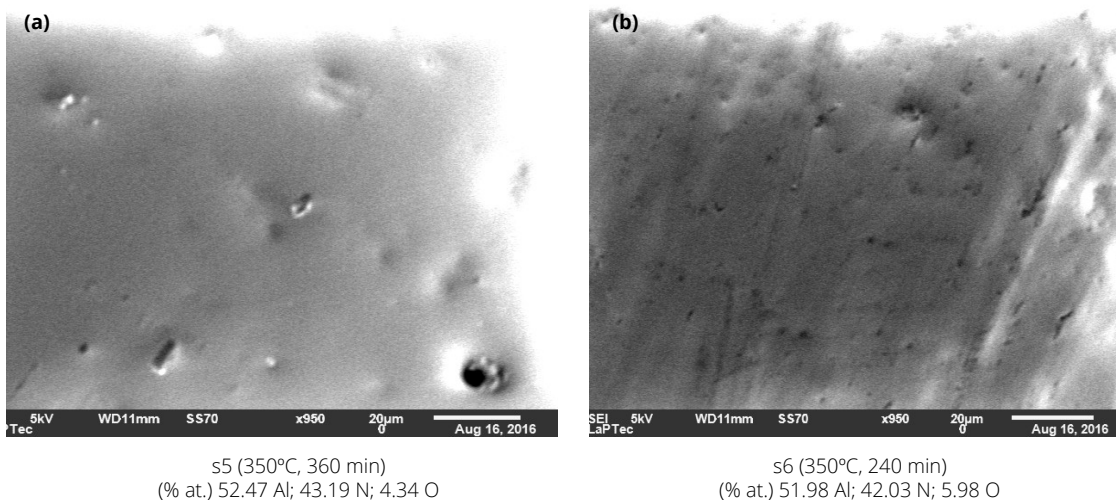


Figure 4: Scanning electron microscopy images for aluminum nitride (AlN) samples 5 (a, s5) and 6 (b, s6) generated at 2 kV, $\times 950$ magnification, 20-micron area and 11-mm working distance.

The presence of the heating of the external source on sample 4 did not result in films with values of proportion of elements different from the other films, being predominant to the orientation character of the crystalline planes, and of nucleation in the first stages. It affects the proportion of elements in the structure of the thin films, whose proportion of Al varied between 51.57 and 51.98 (% at.), while the proportion of N varied between 42.03 and 43.6 (% at.). The presence of oxygen was detected by the equipment analysis (X-ray dispersive spectroscopy), with proportions between 4.34 and 5.98 (% at.).

It is possible to observe in the images that the thin films were smooth with similar morphology, even with the presence of micropores (dark points of the image) or grains (light points). The thin film from sample 5 was deposited for one hour longer than the film from sample 6, for which the other deposition parameters were kept fixed. This may indicate that films deposited in longer times are freer from structural defects on the surface. It is believed that the highly heated atmosphere for a long time can promote the diffusion of elements that occupy the cavities promoted by the ion bombardment, while the heating by the external source from the first moments of the process can be predominant in the nucleation of the thin film, inherent to the presence of pores, because the ion bombardment took place at the same pressure and RF power.

Note that the AlN thin films deposited at different times (240 and 360 min) were also not different in proportion of elements, being quite homogeneous from the quantitative point of view, since they were well oriented during growth. The films generally incorporate oxygen from the reactor or from the atmosphere, being minimized by the reactor vacuum condition, although the contamination level of the thin films was low, regardless of the deposition parameters.

Considering that the thin films had thicknesses close to or greater than 1 micron, the presence of valleys or peaks formed by tens of few nanometers is constituted by a discrete layer or thickness in relation to the *bulk*.

Raman spectroscopy

The Raman spectroscopy analyses were conducted in a Horiba LabRAM, in order to obtain the Raman displacement as a function of the light intensity of the incident beam. The parameters adopted as input data in the equipment software (LabSpec6) were: 5% of laser intensity in two accumulations, while the duration of the laser interaction with the samples was 10 seconds. An objective lens with 100 times magnification was used, and the intervals of wave numbers for the identification of Raman peaks varied in the condition designated by A, from 50 to 500 cm^{-1} , and in the condition called B, between 550 to 1,200 cm^{-1} . Figure 5A shows the Raman spectra of samples 4, 5 and 6 generated in the first region (A) and Fig. 5B the spectra for region B.

It is reported that all three Raman spectra plotted in region A, represented by Raman displacement in the range of 50 to 500 cm^{-1} , had identical appearance. They showed an intense and acute peak of laser radiation absorption ($\lambda = 514 \text{ nm}$) during Raman scattering. This peak is located close to 315 cm^{-1} , which was attributed to the E2 mode by Carlone and Lakin⁶.

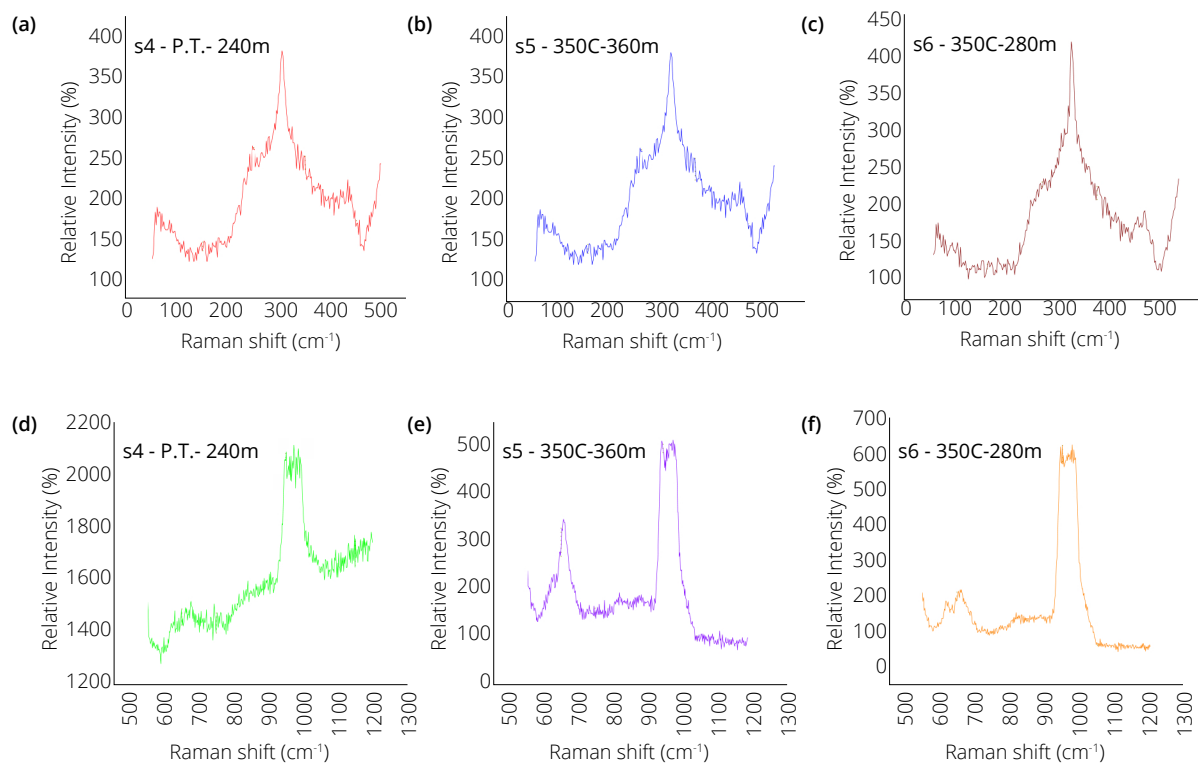


Figure 5: (a, b and c) Raman spectrum of the aluminum nitride (AlN) films of samples 4 (s4) (T.A., 240 min), 5 (s5) (350°, 360 min), and 6 (s6) (350°, 240 min), respectively, for region A of the Raman shift, from 50 to 500 cm⁻¹. (d, e and f): Raman spectrum of the AlN films of samples 4 (s4) (T.A., 240 min); 5 (s5) (350°, 360 min), and 6 (s6) (350°, 240 min), respectively, for the region B of the Raman shift, from 550 to 1,200 cm⁻¹.

The spectrum plotted in region B, represented by Raman displacement in the range of 550 to 1,200 cm⁻¹, revealed peaks similar to each other of high intensity and close to 650 cm⁻¹ (associated with the low frequency component) and in 960 cm⁻¹ of the Raman displacement, confirming the presence of the high intensity of the E1 (LO) vibration mode. These, in turn, are intense peaks with a width close to 60 cm⁻¹ of the Raman displacement.

Table 2 shows the difference in the positions of the peaks obtained in the Raman displacement for some of the AlN thin films, in relation to the theoretical ones, obtained from the literature⁶.

Table 2: Vibration modes observed in Raman shift of aluminum nitride (AlN) films compared to the theoretical ones.

Assignment/modes	A1 (T0)	E ₂ ^z (T0)	E1 (T0)	A1 (LO)	E1 (LO)	E ₂ [']
Experimental (cm ⁻¹)	~615 (sample 6)	657 (samples 5 and 6)	~ 673 (sample 6)	-	Between ~920 e ~980 (samples 4, 5 and 6)	252 (samples 4 and 5)
Theoretical (cm ⁻¹)	615	667	673	881	922	252

Through Tab. 2, it is possible to detect discrete or intense peaks in five polarization modes in the Raman spectra, confirmed by Liu et al.⁷. In its *wurtzitic* form, AlN presents phonons in the center of the Brillouin zone (Γ). With the exception of B1 mode, all optical modes were active Raman modes. The A1 and E1 modes were active infrared (IR) for incident radiation with parallel polarizations and perpendicular to the c plane (for *wurtzite* cells).

Ellipsometry and optical properties

In order to analyze the optical properties of AlN films and evaluate the effects of anisotropy, owing to the preferred films orientation, ellipsometry measurements were made at different angles: 35°, 40°, 50°, 60°, 70° and 80° (angle between normal and the light source or detector), from 300 to 900 nm, for samples 4, 5 and 6.

Therefore, it was feasible to use a (substrate + film) model considering the presence of native oxide (SiO_2) and also a surface roughness effect that the material can present at its interface with the atmospheric air. The idea was to extract through it information about the thickness of the films, gap energy and surface roughness, taking into account that the film is anisotropic in its structural formation.

In this model, the substrate consists of a layer with a large *bulk* of crystalline silicon and a layer of approximately 10 nm of native SiO_2 , whose data were obtained experimentally. The AlN thin films were simulated using the Tauc-Lorentz dispersion formula, present in the database provided by Horiba company. Further on, the surface of the film consisted of a mixture of AlN and void space, called as Void, as can be seen in Fig. 6.

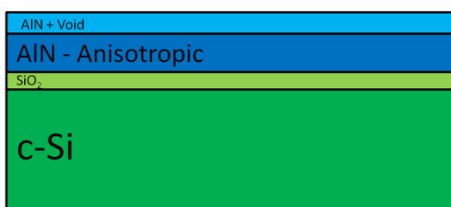


Figure 6: Model (called as Thermox) used to analyze the ellipsometry data of samples 4 (s4) (plasma temperature, 240 min), 5 (s5) (350°, 360 min), and 6 (s6) (350°, 240 min).

In these conditions, the values of refractive indices were for sample 4 $n = 2.1$, for sample 5 $n = 2.4$, and for sample 6 $n = 2.4$.

The thickness values of the AlN films of the samples were $h = 1.2 \mu\text{m}$ for sample 4, $h = 2.0 \mu\text{m}$ for sample 5, and $h = 1.31 \mu\text{m}$ for sample 6, which provided a deposition rate of 5; 8.3; and 5.45 nm/min, respectively.

The gap values of the AlN thin films of the samples were: for sample 4, $E_g = 5.3 \text{ eV}$, for sample 5, $E_g = 4.2 \text{ eV}$, and for sample 6, $E_g = 4.8 \text{ eV}$. The experimental values are lower than the theoretical one, of 6.2. This may have occurred due to the presence of impurities in the film: 4.34 to 5.98% at. oxygen, detected by X-rayDE in these samples. Oxygen atoms (2-) present on the surface were believed to capture loosely bound Si (4+) atoms forming SiO_2 .

Further on, the roughness values of the AlN thin films of the samples were: for sample 4, $R_z = 29 \text{ nm}$, for sample 5, $R_z = 80 \text{ nm}$, and for sample 6, $R_z = 48 \text{ nm}$.

The values revealed that the deposition time has only contributed to increase the thickness of the film, since samples 5 and 6 only differed in this deposition condition. The recorded values of temperature during deposition were very similar or almost identical. For the refractive index and the gap values, they were slightly different between sample 4 (plasma temperature) and sample 5 or 6 (350°).

The films showed a slightly blue color tending to green under visible light. The presence of the heating source in the reactor promotes films with more defined crystallographic direction in the plane (002), which stimulates more rough films, slightly thicker, but with a smaller optical gap than those ones grown without a heating system.

Still on the results of ellipsometry, the AlN films of samples 4, 5 and 6 showed homogeneity of 95% for the bulk of the film against 5% of anisotropy. The increase in deposition time has contributed to obtain thicker films with very similar structural properties. The increase in the nitrogen proportion in plasma in relation to argon was useful to increase the deposition rate of the films, but with gap values lower than the ones obtained in previous periods.

Simulation using COMSOL Multiphysics v.4.3.189

Based on the model seen in references^{8,9}, simulations of a piezoelectric device operating under the principle of surface acoustic waves in a harmonic oscillator containing Si and AlN with thicknesses of 1 and 2 μm , generated, respectively:

- resonance frequency $F_{1\mu\text{m}} = 31.8 \text{ kHz}$, and oscillation amplitude $H_{1\mu\text{m}} = 0.4304 \mu\text{m}$;
- resonance frequency $F_{2\mu\text{m}} = 32.26 \text{ kHz}$, and oscillation amplitude $H_{2\mu\text{m}} = 0.038 \mu\text{m}$.

Figure 7 shows the interface obtained via COMSOL for the two simulated films, providing film thickness (h): (A) AlN $h = 1 \mu\text{m}$, and (B) AlN $h = 2 \mu\text{m}$.

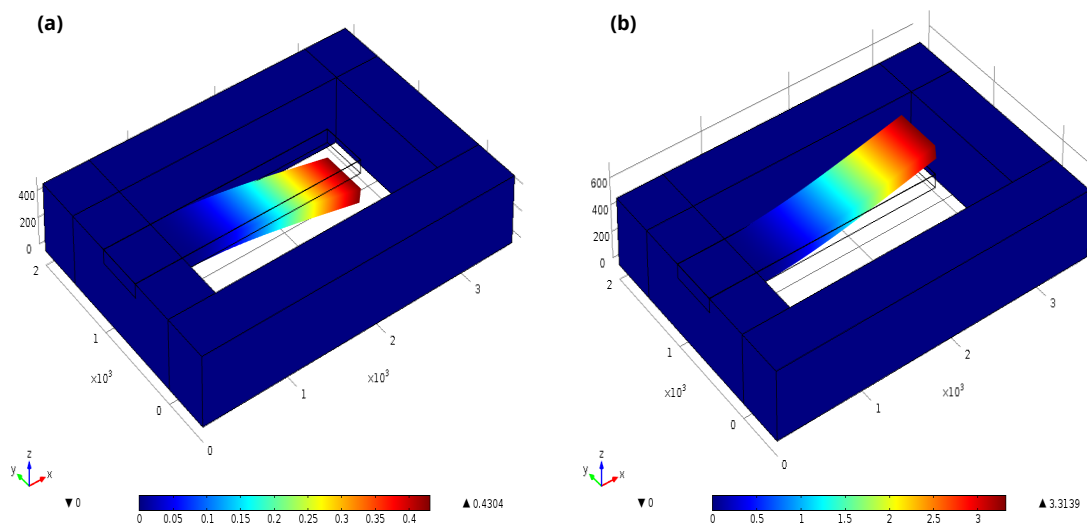


Figure 7: A simple beam embedded in an oscillator operating in the range of a few tens of kHz. Aluminum nitride (AlN) films with thicknesses of (a) 1 μm , and (b) 2 μm . In this compilation, the amplitudes of the oscillator composed of silicon + AlN increased an order of magnitude (from ~ 0.04 to 0.4 μm), when the film doubled in thickness (from 1 to 2 μm).

Still on the simulation, thicker films obtained even lower operating frequencies ~ 19.32 to ~ 21.56 kHz, respectively, for 4 and 9 μm films. In all cases, an increase in the resonance frequency with increasing AlN deposition thickness was detected. The change from single beam to double embedded beam, in this case, without seismic mass allows multiplying the resonance frequency by four times, while using seismic mass it becomes 5.7 times, in all cases for the same deposition thickness.

With respect to structural properties and growth mechanisms, the simple shape indicates a uniformly developed texture over the volume of the film, while a more complex shape suggests the presence of well-textured regions, that is, columns with aligned grains producing a sharp crest in around the specular position, incorporated in a randomly oriented matrix. Each of the axial hexagonal textures with the c axis perpendicular to the substrate was detected in AlN films deposited on silicon^{10,11}. For shorter deposition times, the growth exponent β value less than one unit indicates that a stabilization mechanism during growth is operating, such as surface diffusion or lateral growth¹², consistent with the shadow effect during evolution of the films. The second growth regime for films is not explained by any growth model, owing to variations in crystallinity in polycrystalline films¹³.

Naturally, the value of the surface roughness of films changes with time of growth: $R \propto t^\beta$, in which β describes the process of increasing the roughness of the thin film concomitantly with the growth of the films in the perpendicular direction to the substrate plane¹⁴. The *thickening* process of the films, on the other hand, is associated with the average grain size of the granular structures on the substrate surface, which grows with t , according the relationship $\tau \propto t^{1/2}$. In this case, $1/z$ is known as thickening exponent (*coarsening*), and describes how the granular structure grows on a flat substrate¹⁴. In the case of magnetron sputtering synthesis, the presence of the following predominant mechanisms is expected during the growth stages of AlN thin films:

- Shadowing mechanism: shading of incident particles deposition. This produces a surface with a columnar or granular structure. It is believed to be predominant in AlN films investigated under some specific conditions: over sample 3 (350°C, 240 min) and over sample 4 (plasma temperature, 240 min);
- Surface diffusion mechanism: smooth surfaces, allowing the mobility of atoms adsorbed on the surface.

Therefore, it is suggested for future works the inclusion of atomic force microscopy (AFM) images to estimate the exponent values β for AlN thin films deposited in this plasma condition, not depending *a priori* on the deposition time, which has basically contributed to change the thickness of the films deposited at the same temperature condition throughout the process. The formation of clusters by shadowing is common to stimulate uniform grains and, thus, to contribute to a similar nucleation rate throughout the sample area, especially if the substrate has low to moderate roughness. The evolutionary phase of nucleation is important to define the crystallographic plane to be obtained.

It was possible to determine the orientation direction associated with the texture of the films (002) with diffraction peaks obtained for $2\theta = 36.6^\circ$. For this texture, there is a reduction in the defects of the grain contours stimulating a preferential growth in the crystallographic direction (002). It has been reported that this orientation tends towards the lowest possible surface energy^{15,16}, among which it can be a driving force for the evolution of the texture of the obtained films.

For deposition of temperatures up to 300°C, there is sufficient energy available for the formation of nucleation and growth in the preferred direction, as evidenced by XRD. For temperature values above 300°C, the mobility of atoms increases, as does the length of the surface diffusion towards active sites on the plane (002), as observed in previous works^{17,18}.

Regarding the deposition rates of the films of samples 4 (5 nm/min | grown at room temperature), 5 (8.3 nm/min) and 6 (5.45 nm/min), both samples grown in a sample holder heated to 350°C. The temperature increasing was expected to contribute to the reduction of deposition rates, owing to increased desorption and re-evaporation of atoms from the surface of the films¹⁸. Another possibility of reducing the deposition rate would be associated with an increase in the density of the film with an increase in the substrate temperature¹⁹. However, as the films have more than one crystallographic direction (polycrystalline), it is believed that there are at least two stages of evolution in the growth of the films and, therefore, the deposition rate is not constant.

What actually happens is that, in the heated atmosphere, the vibration of atoms close to the surface generates waves of heat propagation that stimulates greater movement or freedom degrees, which can cause greater interaction between Al and N atoms, with considerable recombination, being then preponderant in relation to desorption or re-evaporation. No model has been found to elucidate the deposition versus desorption events as a function of temperature. Therefore, it was assumed that in crystalline materials chemical bonds are strong and cohesive enough to resist high evaporation and that AlN is not yet formed in the plasma phase, in which the exact temperature is unknown.

On the surface, it is known that atomic disorder is greater. This fact explains the loss of optical properties, such as n and E_{04} in relation to the ideal film, but it does not prevent performance, when simulated in COMSOL, justifying the investment and motivation of this article.

Table 3 summarizes the main properties found in the films according to the deposition parameters: pressure, temperature, RF power, and gas proportion, for all deposition series.

Table 3: Comparison of the behavior or trend of the films depending on the deposition parameters.

Reactor working pressure: fixed at 2 mTorr	Radiofrequency discharge power: 200 to 300 W
Four of the 20 films were deposited under pressure above 2 mTorr, and there was a trend to metallize the film (excess of aluminum), but this parameter has not been decisive for obtaining films with desired properties, keeping fixed the work pressure at 2 mTorr for that the other parameters were checked. At 2 mTorr, it was possible to obtain films with good homogeneity, optical gap above 4 eV and low to moderate roughness (~ 30 to 80 nm) and deposition rate of ~5 nm/min.	At higher powers, there was a tendency to metallize the film (excess of aluminum), or even cause delamination. At 200 W, however, it was possible to obtain more homogeneous films in terms of their proportion of elements, with an oxygen presence of ~5%. The deposition rate of these films were close, ~5 nm/min, optical gap above 4 eV, low or moderate roughness, keeping fixed, and the working pressure of 2 mTorr inside the reactor.
Proportion/flow of argon (Ar) and nitrogen (N ₂) gases	Temperature during depositions
Films deposited with an equal proportion of Ar / N ₂ proved to be fragile with improper structural properties; there was delamination. Better trends were observed with higher concentrations of Ar compared to N ₂ (8:2 or 7:3), with preferential growth in the plane (002), high optical gap and 95% homogeneous part, with the same rough films Rz.	The heating by an external source (~350°C) caused slightly more rough films, with a slightly higher deposition rate, but with a gap slightly below 5 eV, in which higher values were expected. This parameter does not change the proportion of elements in the films, but it was shown to be significant for growing films in the preferential plane (002).

In general terms, the results were consistent, making possible to understand the factors that satisfactorily assisted the properties of the films presented. The strategy of depositing hexagonal AlN films in a heated sample holder and at different process times was useful to the analyses and generated an interesting sequence of experimental evidence. Even with the use of a diffusing pump in the system, the films showed oxygen contamination levels up to ~5% at., substantially reducing the refractive index between 2.1 and 2.4 with optical gap between 4.2 and 5.3 eV, and roughness between ~ 30 and 80 nm.

The temperature influences the deposition rate, which varied between ~5 to 8 nm/min. In this case, these values are considered to be the results of the diffusion and desorption effects of atoms (Si, O, Al and N) and of the *shadowing* and *coarsening* mechanisms, which did not prevent the deposition of thick films (1 to 2 μm) of hexagonal AlN *wurtzites*, grown perpendicular to the preferred plane (002) with granular structures of size $\tau \sim 1.03 \mu\text{m}$, which is oriented in the c-axis direction in polycrystalline form since the XRD detected $\sim 27^\circ$ peaks, associated to an unknown crystallographic direction.

It is worth noting that the best condition was observed in sample 4 (lowest n , highest E_{04} and lowest R_z). Then, adjustments in growth conditions for samples 5 and 6, which grew in a heated sample holder, revealed an inadequate condition to optimize the optical properties (higher n , lower E_{04} and higher R_z). Finally, the effect of temperature on the morphological evolution of the films did not influence the values of oscillation frequency in the simulated harmonic circuit in COMSOL in the order of ~ 30 kHz, suitable for the manufacture of MEMs devices on a large scale. In future analyses, it is recommended: to build a model taking into account the etching of Si.

CONCLUSIONS

This work included the deposition and analysis of six AlN thin films deposited on Si (100). There was growth in the preferred crystalline direction (002) with granular texture perpendicular to the direction plane of the substrate. The temperature difference between the sample holder has little relevance in the deposition rate, and the degree of disorder of the system does not affect the low to moderate roughness of the films (~ 40 to 80 nm). These films presented a gap of 4.2 to 5.3 eV, refractive indexes above 2 and thicknesses above 1.2 μm for deposition times of up to 360 min. The presence of contaminating oxygen was low, around 5% at., which does not prevent the formation of well-oriented structures at long range.

Therefore, even under different growth conditions, there are similarities in the structural properties of the films. In view of these characteristics, the RF sputtering technique is recommended for obtaining films and the simulation in piezoelectric sensors for making MEMs devices based on surface acoustic waves, operating with frequencies of tens of kHz in piezoelectric devices and oscillation amplitude greater than a few hundred nanometers.

AUTHOR'S CONTRIBUTION

Formal Analysis and Funding Acquisition: Leite ASD; **Investigation:** SantAna P, Cezar J; **Methodology:** Leite ASD, Pereira ALJ; **Project Administration:** Sobrinho ASS, Leite ASD; **Software:** Gomes NAS; **Supervision:** Leite ASD; **Validation:** Pericles SantAna P, Cezar J; **Visualization:** SantAna P, Cezar J; **Writing – Original Draft Preparation:** SantAna P; **Writing – Review & Editing:** SantAna P.

DATA AVAILABILITY STATEMENT

Data sharing is not applicable.

FUNDING

Coordenação de Aperfeiçoamento de Pessoal de Nível Superior
<https://doi.org/10.13039/501100002322>
Finace Code 001

ACKNOWLEDGEMENT

Physics Department of Instituto Tecnológico de Aeronáutica, for the opportunity.

REFERENCES

1. Lambrecht W. Electronic structure of diamond, silicon carbide, and the group-III nitrides. *Mater Res Soc Symp Proc.* 1994;339:565. <https://doi.org/10.1557/PROC-339-565>
2. Engelmark F, Fuentes G, Katardjiev IV, Harsta A, Smith U, Berg S. Synthesis of highly oriented piezoelectric AlN films by reactive sputter deposition. *J Vac Sci Technol A.* 2000;18:1609. <https://doi.org/10.1116/1.582394>
3. Dubois M-A, Muralt P. Stress and piezoelectric properties of aluminum nitride thin films deposited onto metal electrodes by pulsed direct current reactive sputtering. *J Appl Phys.* 2001;89(11):6389. <https://doi.org/10.1063/1.1359162>
4. Patterson L. The Scherrer formula for X-ray particle size determination. *Phys Rev.* 1939;56:978. <https://doi.org/10.1103/PhysRev.56.978>
5. Trolrier-McKinstry S, Muralt P. Thin film piezoelectrics for MEMs. *J Electroceramics.* 2004;12(1-2):7-17. <https://doi.org/10.1023/B:JECR.0000033998.72845.51>
6. Madelung O. Physical data (eds) Semiconductors. *J Appl Phys.* 1954;55:4010. https://doi.org/10.1007/978-3-642-97675-9_2
7. Liu MS, Nugent KW, Praver S, Busill A, Peng JL, Tong YZ, et al. Micro-Raman scattering properties of highly oriented AlN films. *Int J Mod Phys.* 1998;12(19):1963-74. <https://doi.org/10.1142/S0217979298001137>
8. Yu J-C, Lan C-B. System modeling of microaccelerometer using piezoelectric thin films. *Sens Actuators A.* 2001;88(2):178-86. [https://doi.org/10.1016/S0924-4247\(00\)00502-1](https://doi.org/10.1016/S0924-4247(00)00502-1)
9. Wang Q-M, Yang Z, Li F, Smolinski P. Analysis of thin film piezoelectric microaccelerometer using analytical and finite element modeling. *Sens Actuators A.* 2004;113(1):1-11. <https://doi.org/10.1016/j.sna.2004.02.041>
10. Akiyama M, Xu CN, Hagio T, Nokana K. Influence of target material by spraying on crystallinity and orientation of thin aluminum nitride film. *J Ceram Soc.* 2002;110(1278):115-7. <https://doi.org/10.2109/jcersj.110.115>
11. Xu X-H, Wu H-S, Zhang C-J, Jin Z-H. Morphological properties of AlN piezoelectric thin films deposited by DC reactive magnetron sputtering. *Thin Solid Films.* 2001;388(1-2):62-7. [https://doi.org/10.1016/S0040-6090\(00\)01914-3](https://doi.org/10.1016/S0040-6090(00)01914-3)
12. Barabasi AL, Stanley HE. Fractal concepts in surface growth. Cambridge: Cambridge University Press; 1995.
13. Kardar M. Dynamic scaling phenomena in growth processes. *Phys B.* 1996;221(1-4):60-4. [https://doi.org/10.1016/0921-4526\(95\)00905-1](https://doi.org/10.1016/0921-4526(95)00905-1)
14. Auger MA, Vázquez L, Jergel M, Sánchez O, Albella JM. Structure and Morphology evolution of AlN films grown by DC sputtering. *Surf Coat Tech.* 2004;180-181:140-4. <https://doi.org/10.1016/j.surfcoat.2003.10.054>
15. Clement M, Iborra E, Sangrador J, Sanz-Hervás A, Vergara L, Aguilar M. Influence of sputtering mechanisms on the preferred orientation of aluminum nitride thin films. *J Appl Phys.* 2003;94(3):1495-500. <https://doi.org/10.1063/1.1587267>
16. Ohuchi S, Russel PE. AlN thin films with controlled crystallographic orientations and their microstructure. *J Vac Sci Technol A.* 1987;5:1630. <https://doi.org/10.1116/1.574579>
17. Ohring M. The materials science of thin films. San Diego: Academic Press; 1992.
18. Chiu K-H, Chen J-H, Chen H-R, Huang R-S. Deposition and characterization of reactive magnetron sputtered aluminum nitride thin films for film bulk acoustic wave resonator. *Thin Solid Films.* 2007;515(11):4819-25. <https://doi.org/10.1016/j.tsf.2006.12.181>
19. Mahmood A, Andrade E, Muhl S, Shah A, Khizar M, Raja MYA. Ion beam analysis of sputtered AlN films. *Curr Appl Phys.* 2011;11(2):182-7. <https://doi.org/10.1016/j.cap.2010.07.003>